Frontiers in Bioscience Elite

Front. Biosci. (Elite Ed) **2026**; 18(2): 44093
https://doi.org/10.31083/FBE44093

Original Research

Bactericidal Action and *in Vitro* Immunomodulatory Effects of Ozone on Methicillin-Resistant *Staphylococcus Aureus*

Cintia Carella[1], Valentina La Sorsa[2], Iole Macchia[3], Sara Giancristofaro[4], Michela Pagnotta[4], Donatella Pietraforte[1], Massimo Sanchez[1], Maurizio Zini[1], Giada Cairo[4], Monica Fabiani[4], Monica Monaco[4], Maria Del Grosso[4], Romina Camilli[4], Giulia Errico[4], Sergio Pandolfi[5], Luigi Valdenassi[5], Marianno Franzini[5], Alessandra Cenci[1,*]

[1]Core Facilities, Italian National Institute of Health, 00161 Rome, Italy
[2]Research Coordination and Support Service, Italian National Institute of Health, 00161 Rome, Italy
[3]Department of Oncology and Molecular Medicine, Italian National Institute of Health, 00161 Rome, Italy
[4]Department of Infectious Diseases, Italian National Institute of Health, 00161 Rome, Italy
[5]Italian Scientific Society of Oxygen Ozone Therapy (SIOOT), Bergamo and High School Master of Oxygen Ozone Therapy, University of Pavia, 27100 Pavia, Italy
*Correspondence: alessandra.cenci@iss.it (Alessandra Cenci)

Academic Editor: Adem Gharsallaoui
Submitted: 20 June 2025 Revised: 8 October 2025 Accepted: 24 November 2025 Published: 5 June 2026

Abstract

Background: Methicillin-resistant *Staphylococcus aureus* (MRSA) poses a major challenge in clinical settings due to limited susceptibility to conventional antibiotics. Ozone (O_3), a naturally occurring molecule composed of three oxygen atoms, exhibits strong antimicrobial properties against a wide spectrum of microorganisms, including both Gram-positive and Gram-negative bacteria. The antibacterial efficacy of O_3 against pathogenic bacteria has been demonstrated both *in vivo* and *in vitro*, although the mechanisms of action remain poorly understood. Notably, O_3 has proven effective against MRSA, underscoring the potential of O_3 as a valuable adjunctive therapy for managing resistant bacterial infections. **Aims**: This study aimed to confirm the antibacterial effects of oxygen–O_3 (O_2–O_3) therapy on MRSA strains and to investigate the associated immunomodulatory and antioxidant properties in human peripheral blood mononuclear cells (PBMCs) treated *in vitro* with MRSA. **Methods**: PBMCs from healthy donors were initially exposed to heat-killed or O_3-treated MRSA strains at 37 °C for 2 hours, then treated with 40 µg/mL O_3 for an additional 24 hours to simulate O_3 therapy. Subsequently, cytokine release, antioxidant and pro-oxidant gene expression, reactive oxygen species production, and redox-related biomarker levels were assessed. **Results**: Our findings demonstrated that O_3, at various concentrations (20–60 µg/mL) within the therapeutic range (20–80 µg/mL), exerts a potent antibacterial effect against MRSA, resulting in complete loss of bacterial colonies, in the absence of antioxidants in the medium. Using a multidisciplinary approach encompassing biochemical, molecular, and cell biology techniques, we observed that O_3 exerts immunomodulatory and antioxidant effects on PBMCs exposed to O_3 and stimulated with MRSA as early as 1 hour after stimulation, with these effects persisting for up to 48–72 hours, regardless of whether the bacteria were inactivated by O_3 or heat. **Conclusions**: We successfully demonstrated that O_3 exerts an early antibacterial effect, followed by antioxidant activity and immunomodulatory properties, as confirmed by multiple integrated analyses. These findings highlight the potential of O_3 as a promising strategy to combat antibiotic resistance and support therapeutic protocols.

Keywords: ozone; methicillin-resistant *Staphylococcus aureus*; cytokines; immune response; antioxidants, anti-inflammatory agents

1. Introduction

Antimicrobial resistance (AMR) is a growing global health concern underscoring the urgent need for innovative therapeutic approaches and robust antimicrobial stewardship (WHO 2023, https://www.who.int/news-room/fact-sheets/detail/antimicrobial-resistance) [1,2].

Among resistant pathogens, methicillin-resistant *Staphylococcus aureus* (MRSA) remains a major clinical challenge causing infections ranging from minor skin conditions [3] to severe systemic diseases such as sepsis, endocarditis, and pneumonia [4,5].

Ozone (O_3), a triatomic oxygen molecule, has historically been used for water disinfection and the topical treatment of wound infections [6].

When properly administered, oxygen–O_3 (O_2–O_3) therapy is considered safe and non-toxic, as shown by *in vivo* studies [7]. At low concentrations (≥20 µg/mL), O_3 exhibits potent bactericidal activity against Gram-positive and Gram-negative bacteria, particularly against antibiotic-resistant strains [8–11].

Moreover, O_3 has been shown to potentiate the antimicrobial efficacy of antibiotics such as vancomycin against MRSA by increasing cell wall permeability and inhibiting

Copyright: © 2026 The Author(s). Published by IMR Press.
This is an open access article under the CC BY 4.0 license.

Publisher's Note: IMR Press stays neutral with regard to jurisdictional claims in published maps and institutional affiliations.

biofilm formation [12–14]. In addition to the antibacterial properties of O_3, antiviral efficacy has been demonstrated against Herpes zoster [15], Herpes simplex [16], and SARS-CoV-2, primarily through viral load reduction and immunomodulation via the regulation of cytokine signaling [17–24].

Moreover, O_3 therapy within the therapeutic range of 20–80 µg/mL has been shown to exert immunomodulatory and antioxidant effects that contribute to the overall associated antimicrobial potential [25–27].

Meanwhile, O_3 exhibits antibacterial activity through both direct and indirect mechanisms. The direct antibacterial effects of O_3, relevant primarily to *in vitro* applications and surface disinfection, occur through three main pathways: (a) induction of oxidative stress in bacterial cells leading to lipid peroxidation and membrane damage, culminating in cell lysis [26–29]; (b) oxidation and inactivation of essential bacterial enzymes, thereby disrupting key metabolic functions [30,31]; (c) oxidative damage to bacterial DNA, impairing replication and repair processes, and inhibiting bacterial proliferation [32].

In addition, O_3 may exert indirect antibacterial activity *in vivo* through immunomodulatory mechanisms, by stimulating cytokine release and immune cell activation [28,29], enhancing host defense mechanisms against microbial infections [31–34].

Upon administration, medical O_3 rapidly reacts with lipids, generating reactive oxygen species (ROS) including hydrogen peroxide (H_2O_2) and lipid peroxides (LOPs). This reaction leads to the formation of 4-hydroxynonenal (4-HNE), a key lipid peroxidation product of ω-6 polyunsaturated fatty acids (PUFAs), which activates the nuclear factor erythroid 2-related factor 2 (NRF2)-mediated adaptive response [35].

In both *in vivo* and *in vitro* models, exposure to low O_3 concentrations induces mild intracellular and mitochondrial oxidative stress–triggering hormetic and mitohormetic signaling through the NRF2–Keap1–ARE pathway [36–39]. ROS generated by O_3, also activate the NRF2, which translocates to the nucleus and binds antioxidant response elements (AREs) in complex with MAF transcription factors, inducing the expression of antioxidant and anti-inflammatory genes, including superoxide dismutase (*SOD*), catalase (*CAT*), glutathione peroxidase (*GPx*), glutathione reductase (*GR*), glutathione-S-transferase (*GST*), NAD(P)H quinone dehydrogenase 1 (*NQO1*), heme oxygenase 1 (*HO-1*) and the thioredoxin/thioredoxin reductase system (*TXN/TXNRD*) [37,40]. Simultaneously, NRF2 activation suppresses the nuclear factor kappa-light-chain-enhancer of activated B cells (NF-κB) signaling, thereby reducing the expression of pro-inflammatory cytokines [41].

Additionally, O_3 may reduce inflammation through two complementary mechanisms: first, it prevents the activation of the NLR family pyrin domain-containing 3 (NLRP3) inflammasome, a key driver of interleukin-1β (IL-1β) and interleukin-18 (IL-18) release, meanwhile NF-κB independently promotes IL-6 and TNF-α production [42,43]. In parallel, O_3-induced NRF2 activation decreases these pro-inflammatory cytokines and promotes IL-10 expression potentially contributing to the activation of regulatory T cells (Tregs) that support immune homeostasis [43–45].

Thus, this study aimed to explore the mechanisms underlying the *in vitro* action of O_3 against MRSA. We first examined the effect of O_3 on MRSA viability, and then, using an integrated biochemical, cellular, and molecular approach, investigated the immunomodulatory and antioxidant effects of O_3 on PBMCs as a human-relevant model. Specifically, we assessed cytokine production by PBMCs stimulated with O_3 or heat-inactivated MRSA and subsequently treated with O_3 to evaluate ozone anti-inflammatory and redox homeostasis–restoring properties. These effects were studied, in a time-dependent manner, by assessing the: (i) production of pro-inflammatory cytokines using a Cytokine Bead Array (CBA) to detect TNF-α, IL-1β, IL-8 and IL-10 and intracellular cytokine staining (ICS) for IFN-γ, IL-4, IL-10 and IL-17; (ii) the expression of inflammatory (*NLRP3, NFKB1 and NFKB2*) and antioxidant (*NFE2L2*) genes using quantitative real-time polymerase chain reaction (qRT-PCR); (iii) intracellular redox status, by measuring ROS release, glutathione concentration and the activity of the antioxidant enzyme Gpx.

Our findings demonstrated that O_3 exerts both direct antibacterial effects against MRSA and potent immunomodulatory and antioxidant actions on human PBMCs. By activating the NRF2 pathway and suppressing key inflammatory mediators, O_3 promotes redox homeostasis and an anti-inflammatory cellular phenotype, supporting the potential use of O_3 as an adjunctive therapeutic strategy for antimicrobial-resistant infections.

2. Materials and Methods

2.1 O_3 Generation and Monitoring

The experiments were conducted employing the MEDICAL 99 IR Multiossigen device (Gorle, Bergamo, Lombardy, Italy), provided by SIOOT. The device is certified by the Notified Body of the Ministry of Health as Class IIa under Directive 93/42/EEC.

2.2 Bacterial Strains

For the experiments, we used the MRSA USA300 reference strain from our collection of isolates derived from clinical specimens. The growth and inactivation of MRSA were conducted in Tryptic Soy Broth (TSB, OXOID) overnight (O/N) at 37 °C. The O/N bacterial culture was diluted 1:100 in fresh TSB broth and incubated until the exponential growth phase was reached (OD_{600} = 0.6). The bacterial culture was then processed using two protocols, namely one-step and multi-step, prior to O_3-

induced bacterial killing. In the one-step approach, 5 mL of the bacterial culture (OD_{600} of 0.6) was washed and resuspended in phosphate-buffered saline (PBS) (*v/v*) before proceeding with O_3 killing. The bacterial culture was treated, in independent experiments, with three O_3 concentrations (20 µg/mL, 40 µg/mL and 60 µg/mL, respectively) for 5 minutes (MRSA O_3I). To verify whether bacterial killing was successful, 10-fold serial dilutions of the bacterial suspension from each treatment condition, were prepared, plated on Tryptic Soy Agar (TSA; Oxoid Ltd., Basingstoke, Hampshire, UK) and incubated at 37 °C O/N. The absence of bacterial growth was taken as evidence of the efficacy of the killing method.

In the multi-step protocol, 5 mL of the bacterial culture (OD_{600} of 0.6), was washed twice in RPMI 1640 and resuspended in ozonated RPMI 1640 (*v/v*) obtained by a prior O_3 treatment at 60 µg/mL for 20 minutes. RPMI 1640 ozonation was necessary to reduce the antioxidant effect of the medium. The bacterial suspension in ozonated RPMI 1640 was subsequently treated with an O_3 concentration of 60 µg/mL at 20-minute intervals for at least 1 hour, depending on the initial bacterial concentration. After O_3 treatment, 200 µL of the bacterial suspension was plated at serial dilutions either on TSA or on Chromid MRSA SMART plates (bioMérieux SA, Marcy-l'Étoile, France) to assess killing activity.

In addition, two further bacterial-killing experiments were performed with a bacterial cell density (10^7 colony-forming units (CFU)/mL) using heat inactivation or gamma-ray irradiation. In the first experiment, the bacterial culture was washed in PBS and heat-inactivated at 100 °C for 10 minutes. In the second experiment, bacterial culture was treated with O_3 for up to five hours according to the multi-step protocol, and the surviving rare colonies were subsequently subjected to gamma-ray irradiation over the weekend at a dose of 2700 Gy [46] as described in more detail in the Results.

Gamma irradiations from a ^{137}Cs source were performed at the Istituto Superiore di Sanità (ISS, Rome, Italy) using the Gammacell Exactor 40 (Nordion) [47].

The MRSA bacterial culture (10^7 CFU/mL) was heat-inactivated at 100 °C, to prepare the control (MRSA HI) [48]. To confirm the lack of viable bacteria following heat inactivation and gamma-ray irradiation, 200 µL of the bacterial suspension was plated on TSA and incubated at 37 °C O/N.

2.3 In Vitro Stimulation of PBMCs

The study was approved by the Ethics Committee of the Italian National Institute of Health (Istituto Superiore di Sanità, ISS), Rome, Italy (Protocol PRE BIO CE n. 0041072, November 24, 2021). Peripheral blood mononuclear cells (PBMCs) were isolated from healthy adult volunteers who provided written informed consent, in accordance with the Agreement between the Umberto I University Hospital (AOU Policlinico Umberto I, Rome) and the ISS regarding the "transfer of blood and its derivatives for laboratory use", established under Resolution No. 0000853 of August 18, 2020. Only primary PBMCs were employed to ensure a physiologically relevant model; no immortalized or transformed cell lines were used.

PBMCs were isolated from buffy coats obtained from healthy donors (n = 3/5) released by the Transfusion Center of Rome Policlinico Umberto I, as previously described [49]. PBMCs were cultured in RPMI 1640 with 10% fetal bovine serum (FBS) and stimulated with MRSA at a multiplicity of infection (MOI) of 1, using bacteria inactivated by the methods that yielded the most effective bactericidal results. After two hours of stimulation, PBMCs were treated with O_3 at 40 µg/mL to investigate, *in vitro*, the immunomodulatory and anti-inflammatory actions observed *in vivo*. Appropriate negative controls and Staphylococcal enterotoxin B (SEB) from Sigma-Aldrich (St. Louis, Missouri, USA; catalog no. S4881) positive controls were included in all experiments, conducted with both MRSA -O_3-inactivated (MRSA O_3I) and MRSA HI bacteria.

Our experiments were conducted using PBMCs isolated from freshly obtained buffy coats, ensuring that blood donations were processed within 24 hours of collection. This short interval between blood withdrawal and PBMC isolation is unlikely to allow the emergence of detectable changes in cellular morphology, surface marker expression, or mycoplasma contamination.

2.4 Detection of Cytokines in Culture Supernatants

Cytokine production (TNF-α, IL-10, IL-6, IL-1β and IL-8) was quantified in culture supernatants collected from PBMCs before and 24 h after stimulation with various bacterial preparations, with or without O_3, as well as from untreated PBMCs. Cell samples were analyzed using a specific Cytometric Bead Array (CBA) Human Inflammatory Cytokine Kit (BD Biosciences, San Jose, CA, USA; cat. BDB551811). Samples were acquired on a FACS Canto II flow cytometer (BD Biosciences, San Jose, CA, USA), and data were analyzed with FCAP Array software v3.0 (BD Biosciences, San Jose, CA, USA) according to the manufacturer's instructions.

2.5 Intracellular Cytokine Staining (ICS)

For intracellular cytokine analysis, we used a dried commercial panel (Duraclone IF T Helper Cell kit #C04666, Beckman Coulter, Brea, CA, USA) as the backbone, supplemented with liquid-format antibodies against CD8, IL-10, and a dead-cell exclusion marker, see Table 1 for details of the antibodies. Briefly, PBMCs from healthy donor buffy coats were cultured under three conditions: unstimulated (NT), stimulated with SEB at 2 µg/mL as a positive control, or stimulated with MRSA HI or MRSA O_3I (at a 1:1 MRSA:PBMC ratio). After 2 hours, samples were treated with O_3 (40 µg/mL or 20 µg/mL) and then incu-

Table 1. ICS T helper flow cytometry panel.

Fluorescence channel	Fluorochrome	Marker	Catalog	Company	Formulation
FL-1	FITC	IFN-γ	C04666	Beckman Coulter	Dried
FL-2	PE	IL-10	501404	Biolegend	Liquid
FL-5	PC7	IL-4	C04666	Beckman Coulter	Dried
FL-6	APC	CD4	C04666	Beckman Coulter	Dried
FL-7	AF700	CD8	344724	Biolegend	Liquid
FL-8	AF750	CD3	C04666	Beckman Coulter	Dried
FL-9	PB	IL-17	C04666	Beckman Coulter	Dried
FL-10	Aqua	LIVE/DEAD™	L34966	Invitrogen	Liquid

Table 1 presents the integrated ICS T helper panel, in which antibodies conjugated to different fluorochromes and directed against specific surface and intracellular markers are listed. FL (Fluorescence channel), fluorochrome, and antibody markers used in the integrated ICS T helper panel. Cells were stained with antibodies targeting surface markers (CD3, CD4, CD8) and intracellular cytokines (IFN-γ, IL-4, IL-10, IL-17), each conjugated to a specific fluorochrome. Fluorochromes included FITC, PE, PC7, APC, AF700, AF750, PB, and LIVE/DEAD™ Aqua viability dye. The manufacturer, catalog number, and formulation for each antibody are indicated in the table. ICS, intracellular cytokine staining; FITC, fluorescein isothiocyanate; PE, phycoerythrin; PC7, phycoerythrincyanin 7; APC, allophycocyanin; AF, Alexa Fluor; PB, Pacific Blue; IFN-γ, Interferon-gamma; IL, interleukin; CD, Cluster of Differentiation.

bated for 24 hours with Brefeldin A and Monensin (Becton Dickinson), which were added ~1-hour post-O_3 treatment.

The next day, cells were stained for dead cell exclusion, followed by staining with the Duraclone antibody cocktail, which incorporated anti-CD8 and anti-IL-10 monoclonal antibodies. Samples were acquired on a FACS Gallios instrument (Beckman Coulter, Brea, CA, USA), and data were analyzed using the Kaluza Analysis Software v.1.3 (Beckman Coulter Brea, CA, USA).

The gating strategy for multiparameter intracellular cytokine analysis within the CD3+, CD4+, and CD8+ T gates is shown in **Supplementary Fig. 1**, beginning with singlet and live-cell selection followed by T cell subset identification and cytokine detection (IFN-γ, IL-4, IL-17 and IL-10). Representative dot plots are shown for CD3+ T cells under NT and SEB-stimulated conditions. The same analysis was applied to CD4+ and CD8+ T cells as well as to samples treated with MRSA alone and MRSA + O_3.

2.6 RNA Isolation and qRT-PCR Analysis

Total RNA was isolated from 3 $\times$ 10^6 PBMCs, either untreated or stimulated for 24, 48 or 72 hours with MRSA HI or MRSA O_3I and subsequently exposed to O_3 *in vitro* using TRIzol reagent (Invitrogen, Thermo Fischer Scientific, Waltham, MA, USA). Extracted RNA was quantified with a NanoDrop OneC spectrophotometer (Thermo Fisher Scientific, Waltham, MA, USA), and RNA quality was assessed using an established 260/280 absorbance ratio cutoff of ~1.8. Reverse-transcription was performed using the Vilo reverse transcription kit (Invitrogen, Thermo Fisher Scientific, Waltham, MA, USA). The expression of genes *NFE2L2* (NRF2 protein), *NLRP3* (NLRP3 protein), *NFKB1* and *NFKB2* genes (encoding the inactive precursors p105 and p100 of the NF-κB complex) was measured by qRT-PCR using the corresponding TaqMan assays and TaqMan Universal Master Mix II (Applied Biosystems, Thermo Fisher Scientific, Waltham, MA, USA) on a ViiA7 Instrument (Applied Biosystems, Thermo Fisher Scientific, Waltham, MA, USA). The housekeeping gene *TATA-box-binding protein (TBP)* served as the endogenous normalizer. Real-time reactions were performed at least in duplicate. Sample values for each mRNA were normalized to the selected housekeeping gene using the $2^{-\Delta Ct}$ method.

2.7 ROS Measurement

Among the various methods available to assess ROS production or oxidative stress in cells, we used the probe 2′,7′-Dichloro-dihydro-fluorescein diacetate (DCFH-DA). This is a lipophilic, cell-permeable, non-fluorescent probe that, upon hydrolysis by intracellular esterases, yields DCFH, which fluoresces upon oxidation by intracellular ROS. Oxidation of the probe results from the action of several types of peroxynitrite, hydroxyl radicals, nitric oxide, metal-derived oxidants and other peroxides, and can be detected by flow cytometry. PBMCs were seeded at 1 $\times$ 10^6/mL, and incubated with bacterial preparations including O_3-killed bacteria (20–60 µg/mL O_3) and heat-killed MRSA as a control. After incubation at 37 °C, with 5% CO_2, for 2 hours, we added 2′,7′-Dichlorofluorescein (DCF) (Sigma) to a final concentration of 5 µM to detect intracellular ROS and incubated the cells for at least 1 hour, before the subsequent treatment with 40 µg/mL O_3. We used the MultiOssigen O_3 technology - Medical 99IR (MultiOssigen S.p.a) as an O_3 delivery system.

After ozonation, the samples were centrifuged at 1200 rpm at room temperature for 10 minutes and the pellets were then suspended in PBS containing the vital dye Sytox Blue (Invitrogen™ Cat. n. S34857) at 1:1000 for flow cyto-

metric analysis of ROS using the CytoFLEX LX (Beckman Coulter) with excitation and detection wavelengths of 488 nm and 535 nm, respectively. As negative controls, we used PBMCs and PBMCs plus DCF, with and without O_3 insufflation, to estimate the number of unstained cells with autofluorescence in the green emission range and to quantify basal ROS levels in our sample. As a positive control, we incubated cells with 0.1 mM H_2O_2, with and without O_3 insufflation.

ROS production was assessed every 20 minutes for 2 hours following O_3 administration, with a final measurement taken at 24 hours. The gating strategy for ROS measurement with DCF is described in **Supplementary Fig. 2**.

2.8 PBMC Redox Status Evaluation

PBMCs (2×10^6/mL) were incubated in the absence or in the presence of the different stimuli at 37 °C for 2 hours. O_3 (40 µg/mL) was then added and, after a further 22 hours incubation, cells were washed, resuspended in an appropriate volume of PBS, and lysed (1:2 *v/v*) in RIPA buffer (50 mM Tris HCl, pH 8.0, 150 mM NaCl, 0.5% sodium deoxycholate, 0.1% SDS) containing protease inhibitors (10 µg/mL, leupeptin, 10 µg/mL aprotinin, 0.15 mM PMSF). After 10 minutes in ice, cell lysates were diluted 1:4 (*v/v*) in PBS. An aliquot of cell lysate was treated with ice-cold 20% trichloroacetic acid (1:2 *v/v*) for 10 min on ice, then centrifuged at 15,000 rpm, at 4 °C for 10 min. The cleared acidic supernatants, used for glutathione measurement, and the residual cell lysate volume, used for protein measurement and GPx activity evaluation, were stored at –80 °C and used within one week. The glutathione and the glutathione peroxidase assay kits (Cayman Chemicals) were used to measure glutathione concentration and GPx activity, respectively, according to the manufacturer's instructions. Protein content was measured using the BCA Protein Assay kit (Millipore).

2.9 Statistical Analysis

We computed the between-samples Pearson's correlation coefficients to check the consistency among different subjects (samples) across all the measured variables. The results indicated strong consistency among independent subjects, providing confidence in the reliability of the data (Table 2). Therefore, given the similarity among profiles, we considered the pattern reproducible despite the small sample size (n = 3–5) used. A two-tailed paired Student's *t*-test was then performed according to the experimental design, with $p < 0.05$ considered statistically significant. Raw data are presented in **Supplementary Tables 1,2**.

2.10 Study Limitations

The relatively small sample size in this study is justified by the preliminary nature of the analysis, aimed at exploring specific *in vitro* effects of O_3 exposure. This initial investigation provides valuable insights that can inform the design of future, larger-scale studies to achieve a more comprehensive understanding. While the *in vitro* model does not fully replicate the complexity of living organisms, a useful platform is provided to examine the associated cellular and molecular responses to ozone.

Our choice to use inactivated bacteria was a deliberate methodological decision guided by the primary objective of our study. The aim of the study was not to replicate

Table 2. Pearson correlations.

Techniques	Samples					
DCF	Exp 5	Exp 3	Exp 4	Exp 2	Exp 1	
Exp 5	1	0.905	0.903	0.753	0.840	
Exp 3	0.905	1	0.882	0.680	1	
Exp 4	0.903	0.882	1	0.746	0.703	
Exp 2	0.753	0.680	0.746	1	0.691	
Exp 1	0.840	1	0.703	0.691	1	
CBA	Exp 5	Exp 3	Exp 4	Exp 2		
Exp 5	1	0.857	0.857	0.857		
Exp 3	0.857	1	0.936	0.936		
Exp 4	0.936	0.924	1	0.786		
Exp 2	0.786	0.909	0.856	1		
ICS	Exp 1	Exp 2	Exp 4	Exp 3	Exp 5	
Exp 1 MRSA O_3I	1	0.985	0.985	0.985	0.985	
Exp 2 MRSA O_3I	0.985	1	0.933	0.933	0.933	
Exp 4 MRSA O_3I	0.933	0.949	1	0.873	0.873	
Exp 3 MRSA HI	0.873	0.911	0.863	1	0.741	
Exp 5 MRSA HI	0.741	0.757	0.725	0.786	1	
Redox status	Exp 3	Exp 4	Exp 5	Exp 3	Exp 4	Exp 5
Exp 3 MRSA HI	1	0.937	0.937	0.937	0.937	0.937
Exp 4 MRSA HI	0.937	1	0.920	0.920	0.920	0.920
Exp 5 MRSA HI	0.920	0.990	1	0.980	0.980	0.980
Exp 3 MRSA O_3I	0.980	0.994	0.984	1	0.955	0.955
Exp 4 MRSA O_3I	0.955	0.979	0.962	0.992	1	0.955
Exp 5 MRSA O_3I	0.955	0.979	0.962	0.958	0.958	1
qRT-PCR (24–72 h)	Exp 3	Exp 5	Exp 4			
Exp 3	1	0.788	0.788			
Exp 5	0.788	1	0.422			
Exp 4	0.422	–0.360	1			
qRT-PCR (48–72h)	Exp 3	Exp 4				
Exp 3	1	0.843				
Exp 4	0.843	1				

Table 2 presents Pearson correlation coefficients is a statistical value to assess consistency across subjects (samples) for all measured variables. The range of values goes from 0, which indicates no correlation, to +1 or –1. +1 means that the correlation is maximally positive, so the two variables grow together, while –1 indicates that the correlation is maximally negative, so as one variable grows, the other decreases. MRSA O_3I and MRSA HI are always evaluated, even when not indicated. The coefficient value, close to 1, indicated a strong similarity among independent subjects, providing confidence in the reliability of the data. MRSA O_3I, MRSA O_3-inactivated; MRSA HI, heat-inactivated.

Table 3. MRSA inactivation in three different conditions.

	OD	CFU/mL
PBS single-step (A)	–	–
MRSA O_3I untreated	0.70	7×10^6
MRSA O_3I treated with 20 µg/mL O_3 for 5 min	–	0
MRSA O_3I untreated	0.73	8.7×10^7
MRSA O_3I treated with 40 µg/mL O_3 for 5 min	–	0
MRSA O_3I untreated	0.70	6.4×10^6
MRSA O_3I treated with 60 µg/mL O_3 for 5 min	–	0
HEAT-inactivated (B)		
MRSA HI untreated	0.70	3.7×10^7
MRSA HI treated for 15 min	–	0
RPMI multi-step (C)	–	–
MRSA O_3I untreated	0.60	5.4×10^6
MRSA O_3I treated with 60 µg/mL O_3	–	–
20 min	Not done	7.1×10^4
40 min	Not done	1.1×10^4
60 min	–	0

Table 3 summarizes MRSA inactivation under three experimental conditions: (A) single-step O_3 treatment in PBS, (B) heat inactivation as a control, and (C) multi-step O_3 exposure in RPMI.

an active infection, but to isolate and investigate the direct effect of ozone on the immunomodulatory and antioxidant responses of host cells to bacterial components without the additional complexities and unpredictable variables introduced by live bacterial replication and metabolism. Thus using inactivated bacteria allowed us to isolate specific response mechanisms and ensure reproducibility, which is essential for reliable comparative analysis across experimental groups.

The immunomodulatory effects of O_3 were assessed in PBMCs using functional assays to measure cytokine production, ROS, and oxidative stress. In addition, we performed qRT-PCR analysis on selected pathway regulators including key genes such as *NFKB1*, *NFKB2*, and *NLRP3* (involved in immune activation) at early stages of O_3 treatment, and NRF2 (from gene *NFE2L2*) (associated with antioxidant and anti-inflammatory responses) at a later stage. This approach reflects the hypothesis-driven nature of our study, which focuses on the involvement of well-established genes in immune response, rather than on a broad, data-driven exploration. Meanwhile, qRT-PCR was selected for the associated high sensitivity and accuracy of the assay in quantifying expression changes in the genes of interest, thereby supporting our hypotheses. Although RNA-sequencing could aid broader preliminary analyses, this method was deemed unnecessary for the specific goals of this study.

Together, these functional and molecular evaluations provide robust evidence of the biological impact of O_3. Nevertheless, further studies employing more complex models, larger sample sizes, and *in vivo* validation will be necessary to substantiate and expand upon these findings.

3. Results

3.1 Effects of O_3 on MRSA Survival

The bactericidal activity of O_3 against MRSA was first assessed using a single-step exposure protocol. MRSA suspensions (10^6–10^7 CFU/mL) in PBS were exposed to O_3 for 5 minutes, which was sufficient to achieve maximal bacterial killing (data not shown). For subsequent PBMC stimulation experiments, heat-inactivated MRSA (MRSA HI) was used as a control, providing a non-replicating bacterial stimulus while preserving antigenic properties (Table 3).

When using RPMI medium, a multi-step protocol was implemented to provide a closer clinical replication of relevant exposure conditions. This protocol involves repeated O_3 treatments at 60 µg/mL every 20 minutes, consistent with clinical protocols for managing patients with antibiotic-resistant bacterial infections, where O_3 is administered twice weekly for MRSA treatment [11]. As shown in Table 3C, MRSA suspensions (10^6 CFU/mL) exposed to three sequential O_3 applications over 1 hour exhibited a complete inhibition of bacterial growth.

To further evaluate the efficacy of O_3 in the presence of antioxidant components within RPMI, additional experiments were performed using high-titer MRSA suspensions (10^7–10^9 CFU/mL) and the multi-step exposure scheme. Table 4, summarizes three experiments in which bacterial suspensions were treated every 20 minutes for 3–5 hours. A time-dependent and concentration-dependent logarithmic decline in CFU counts was observed in all cases. After approximately 3 hours of repeated O_3 exposure, a five-log reduction in viable bacteria was achieved, confirming the potent bactericidal effect of O_3 even under conditions that partially mimic physiological environments.

Table 4. Multistep O_3-mediated killing of MRSA in RPMI.

Conditions	CFU/mL
Experiment 1: In 180 minutes from 10^9 CFU/mL	
MRSA untreated	4.3×10^9
MRSA treated with 60 µg/mL O_3	
After 20 min	1.7×10^9
After 180 min	7.6×10^4
Experiment 2: In 300 minutes from 10^9 CFU/mL	
MRSA untreated	6.8×10^9
MRSA treated with 60 µg/mL O_3	
After 100 min	1.2×10^8
After 300 min	1.4×10^4
Experiment 3: In 180 minutes from 10^7 CFU/mL	
MRSA untreated	1.9×10^7
MRSA treated with 60 µg/mL O_3	
After 60 min	1.3×10^4
After 180 min	1.6×10^2

Table 4 presents the results of high-titer MRSA (10^7 to 10^9 CFU/mL) treated with O_3 using a multi-step protocol in RPMI. A time-dependent logarithmic decrease in CFUs was observed in all experiments.

However, at very high bacterial densities, *S. aureus* tends to form aggregates, which can transiently reduce O_3 efficacy due to the protective effect of outer-layer killed cells, meanwhile those within the clusters remain protected, a phenomenon also reported for *Pseudomonas aeruginosa* exposed to conventional antibiotics [50].

To ensure complete sterility before use in stimulation assays with PBMCs, residual bacterial colonies were eliminated by gamma irradiation at 2700 Gy for 3 days. No bacterial growth was observed in any of the preparations after 24 hours. This approach is well documented for decontaminating *S. aureus* in food matrices and has the advantage of preserving protein epitopes, thereby maintaining antigenic integrity [51,52].

Both MRSA-O_3I and MRSA HI preparations were subsequently used to stimulate PBMCs isolated from 3/5 healthy donors.

3.2 Effects of O_3 on Cytokines Released by PBMCs

Cruciani *et al.* [48] showed that *S. aureus* induced a specific panel of regulatory cytokines (IL-23, IL-12, and IL-10) and pro-inflammatory mediators (TNF-α, IL-6, and IL-1β) in human primary dendritic cells, thereby promoting Th1 and Th17 differentiation. To analyze the impact of O_3 treatment on the secreted cytokines, PBMC supernatants were collected after 24 hours of O_3 treatment and stimulation with both MRSA O_3I and MRSA HI (Fig. 1). By CBA (Fig. 1A–E), we observed a reduction in the immunoregulatory cytokines (TNF-α, IL-6, IL-1β, and IL-10) whereas IL-8 slightly increased in the MRSA HI samples. In particular, reductions in IL-1β (Fig. 1B) and IL-6 (Fig. 1C) levels were statistically significant, with p-values of 0.022 and 0.04, respectively, based on experiments performed with PBMCs from four independent donors in the MRSA O_3I group. Stimulation with the SEB positive control induced a significant increase in all tested cytokines compared with the untreated control.

3.3 Effects of O_3 on Intracellular Cytokines Within CD3, CD4 and CD8 Lymphocyte Gates

The intracellular production of cytokines associated with the activation of T lymphocytes was assessed by intracellular cytokine staining in PBMCs stimulated with MRSA O_3I and MRSA HI. The gating strategy is shown in **Supplementary Fig. 1**. A reduction in IFN-γ levels was observed in the CD3+, CD4+, and CD8+ T lymphocyte gated populations following *in vitro* O_3 treatment of MRSA O_3I-stimulated PBMCs, compared with the untreated MRSA O_3I sample. In MRSA HI samples treated *in vitro* with O_3, the decrease in IFN-γ expression in the CD3+ and CD4+ gated populations was considerably less evident (Fig. 2A).

The O_3-induced reduction in IL-4 levels was comparable across all T cell subsets, regardless of the bacterial inactivation method (Fig. 2B).

Conversely, IL-10 was increased in CD3+ and CD8+ T cells following O_3 treatment of cells stimulated with either MRSA O_3I or MRSA HI. In contrast, in lymphocytes in the CD4+ gated population, IL-10 remained unchanged in MRSA O_3I-treated samples, while the IL-10 levels were slightly decreased in the MRSA HI-stimulated samples (Fig. 2C).

An O_3-induced decrease in IL-17 levels was detected exclusively within the CD3+ and CD4+ T cell populations, whereas a slight increase of this cytokine was observed in CD8+ T cells. This trend was consistent across both MRSA strains (Fig. 2D). The increase in IL-17 in CD8+ T cells may be partially correlated with the rise in IL-10 within the same gate in cells exposed to both bacterial strains. Although not statistically significant, these data suggest a trend toward differential expression of intracellular cytokines, except for SEB, which induces a significant increase in all tested cytokines, except IL-17, compared with untreated control samples.

3.4 Effect of O_3 on Inflammatory and Pro-/Anti-Oxidant Genes in PBMCs Treated With MRSA

To assess the effects of O_3 on key regulators of inflammation, we used qRT-PCR to measure the effect of O_3 on prooxidant- *(NLRP3, NF-κB)* and antioxidant NRF2 (*NFE2L2*) gene expressions in PBMCs, treated with MRSA O_3I and MRSA HI and subsequently treated *in vitro* with O_3, compared to unstimulated control cells (Fig. 3).

NRF2 expression, a key regulator of the antioxidant response, increased following O_3 treatment, with the most pronounced upregulation observed after 48 hours in PBMCs exposed to O_3-killed bacteria in PBS and treated with O_3. A more modest increase was noted in cells treated

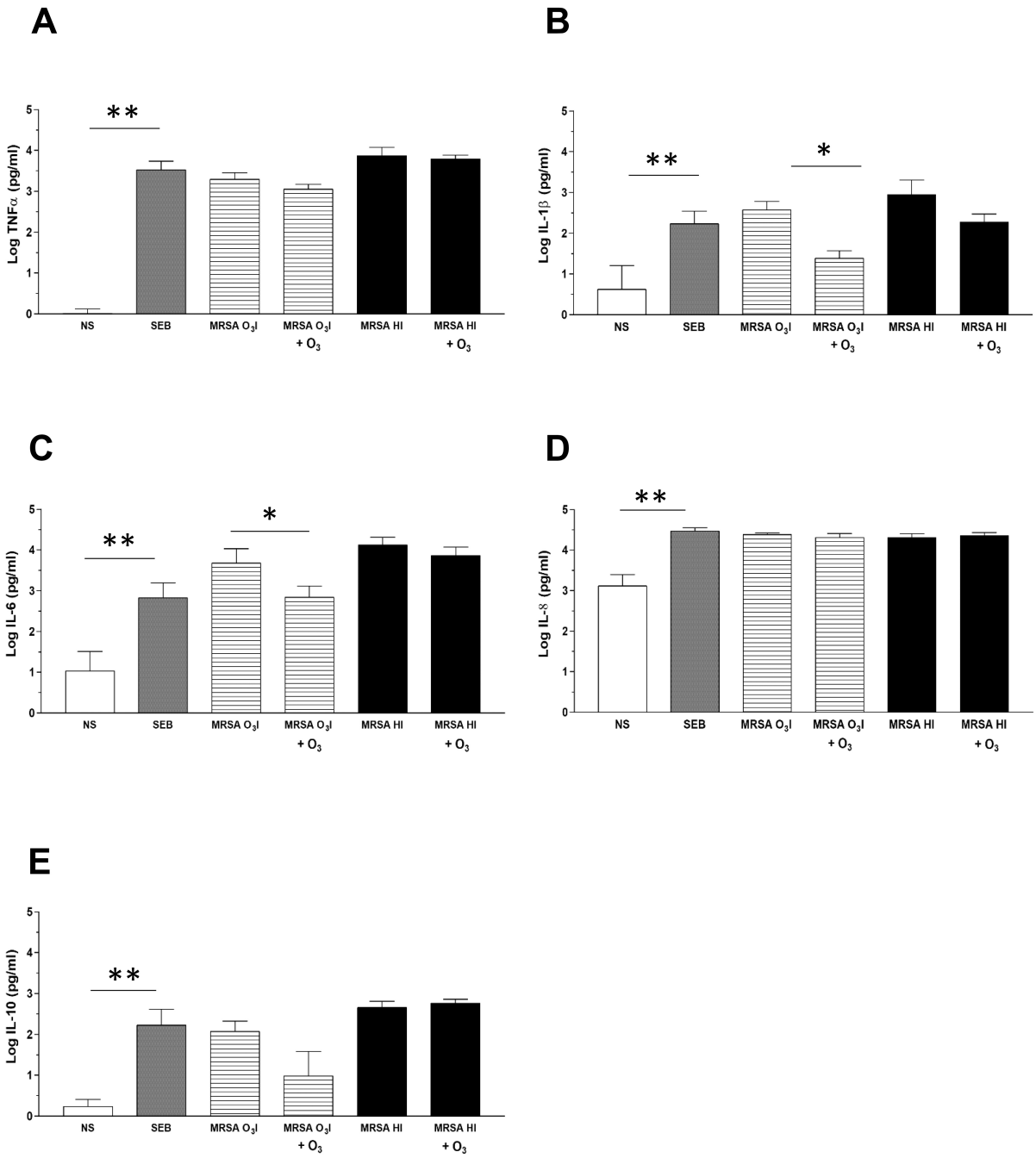


Fig. 1. Cytokine detection in culture supernatants by CBA. The bar graphs depict cytokine levels in culture supernatants from PBMCs collected 24 hours after treatment, with or without O_3 added after 2 hours of stimulation with MRSA O_3I or MRSA HI. Cytokines are expressed in pg/mL on a logarithmic scale. Cytokine production of TNFα (A), IL-1β (B), IL-6 (C), IL-8 (D), and IL-10 (E) was measured over 24 hours using CBA. Negative and positive controls (SEB) were included. Data are presented as the means $\pm$ standard error of mean (SEM) from 4 independent experiments for MRSA O_3I and from 3 independent experiments for MRSA HI (n = 4/3 different healthy subjects). Statistical analysis was performed using paired *t*-tests, with *p*-values indicated (*$p \leq 0.05$, **$p \leq 0.01$, NS, not significant). CBA, Cytokine Bead Array; PBMCs, peripheral blood mononuclear cells; MRSA, methicillin-resistant *Staphylococcus aureus*.

with heat-killed MRSA HI and subsequently exposed to O_3 (Fig. 3A), indicating that O_3 enhances antioxidant defenses, particularly in the context of O_3I bacterial stimulation.

In contrast, *NLRP3*, a proinflammatory gene, was strongly induced by MRSA O_3I at 24 and 72 hours. O_3 treatment attenuated this induction, reducing *NLRP3* expression is reduced to approximately 1.8-fold after 24 hours and decreases further at 48 hours, and by approximately 50% at 72 hours, while a similar reduction was observed in unstimulated cells at 48 hours. PBMCs stimulated with

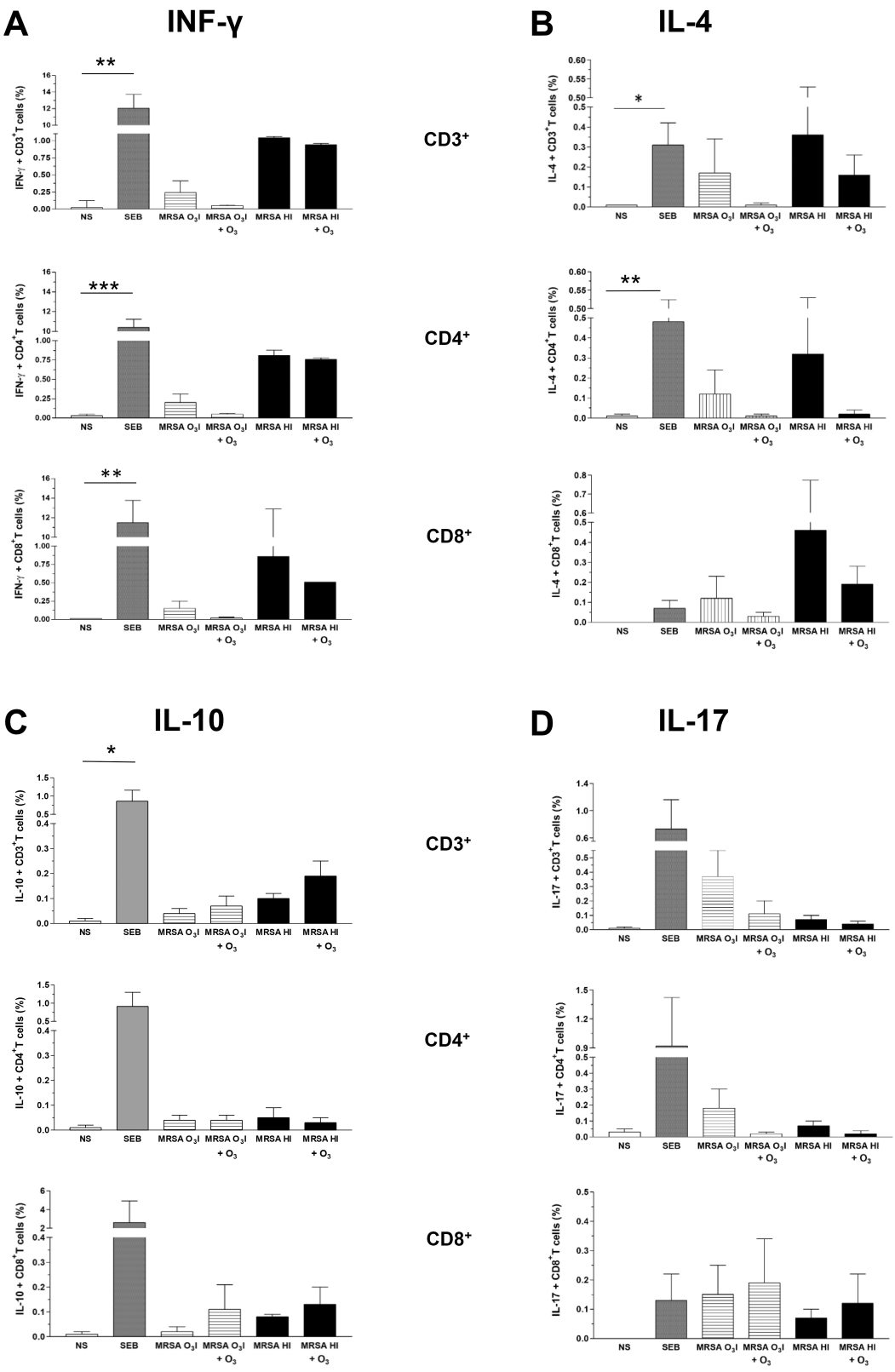


Fig. 2. Intracellular cytokines in CD3, CD4, and CD8 lymphocyte gates. Bar graphs of the percentage of intracellular cytokines IFN-γ (A), IL-4 (B), IL-10 (C), and IL-17 (D), measured by ICS, within CD3+, CD4+, and CD8+ T cell subsets of PBMCs stimulated for 2 hours with MRSA O_3I or MRSA HI, and subsequently treated with O_3 or untreated for 24 hours. Negative and positive controls (SEB) are also included. Data represent the means ± SEM of cytokine-positive cells from three independent experiments with three different healthy subjects for MRSA O_3I and 2 independent experiments with two different healthy subjects for MRSA HI. Statistical significance was determined by paired *t*-test (*$p \leq 0.05$, **$p \leq 0.01$, ***$p \leq 0.001$, NS, not significant). INF-γ, Interferongamma.

MRSA HI showed only minimal changes in *NLRP3* expression (Fig. 3B).

Similarly, *NFKB1* expression induced by MRSA O_3I was affected by O_3 addition at 24 hours and 72 hours while no changes were observed at 48 hours with *NFKB1* below the threshold (Fig. 3C) Likewise, but to a lesser extent *NFKB1* induced by MRSA HI at 24 hours was downregulated by O_3, while no substantial variations in the expression of *NFKB1* were observed in MRSA HI stimulated PBMCs at 48 and 72 hours before and following O_3 treatment. For *NFKB2*, an increase was observed at 24 and 48 hours only in MRSA O_3I stimulated cultures after O_3 treatment, whereas expression decreased at 72 hours. A slight reduction was also measured in MRSA HI-treated PBMCs following O_3 stimulation (Fig. 3C).

NFKB1 expression followed a similar pattern: *NFKB1* was induced by MRSA O_3I at 24 and 72 hours and downregulated by O_3 treatment, whereas at 48 hours expression remained below the threshold. In PBMCs stimulated with *MRSA HI, NFKB1* expression showed only a slight reduction at 24 hours following O_3 exposure, with negligible changes at 48 and 72 hours (Fig. 3C).

Correlation analyses revealed minimal changes in *NFKB1* and *NFKB2* expression at 24 hours, while at 48 and 72 hours, strong correlations were observed among *NRF2*, *NLRP3*, *NFKB1*, and *NFKB2* (Table 2). These findings indicate that O_3 maintains the associated antioxidant and modulatory effects over time, supporting sustained regulation of both pro- and anti-inflammatory pathways for up to 72 hours.

As expected, *NRF2* was not induced by SEB at any time point (24–72 hours), consistent with the role of *NRF2* in anti-inflammatory signaling. Similarly, *NLRP3*, a key component of the inflammasome, was not upregulated at 48–72 hours, suggesting that additional inflammatory stimuli are likely required to induce *NLRP3*. In contrast, the proinflammatory transcription factors *NFKB1* and *NFKB2* were both induced by SEB at 24 and 48 hours. However, by 72 hours, only *NFKB2* remained upregulated, while *NFKB1* returned to baseline levels (**Supplementary Fig. 3**).

Data are presented as the means $\pm$ SEM from three independent experiments up to 24 hours and two independent experiments from 48 to 72 hours. mRNA levels were normalized using the $2^{-\Delta Ct}$ method with GAPDH as the housekeeping gene.

3.5 Effects of O_3 on ROS Production by PBMCs

ROS comprise a wide range of chemical species derived from O_2 that are more reactive than solely O_2, exhibiting distinct properties, reactivities and interactions.

When ROS are generated *in vivo*, numerous antioxidants are activated, delaying, preventing or removing oxidative damage to target molecules [53].

Thus, we evaluated DCF detection in lymphocytes and monocytes separately across the total PBMC population and observed similar kinetics in both cell types within 2 hours and after 24 hours.

As shown in Fig. 4, the presence of the inactivated MRSA in the culture slightly increased the amount of intracellular ROS released by lymphocytes (Fig. 4A) and monocytes (Fig. 4B). Nevertheless, the O_3 treatment initially increased ROS levels, showing an initial oxidant effect of the highly reactive gas. The highest ROS levels were observed within the first 20–40 minutes after ozonation and gradually decreased reaching an antioxidant status comparable to that of the corresponding untreated samples within 2 hours, and even falling below control levels after 24 hours in lymphocytes and monocytes stimulated with MRSA HI, where significant *p* values were found (**Supplementary Table 2**). Meanwhile, a similar trend to MRSA HI was observed for those treated with MRSA O_3I and exposed to O_3 (data not shown). This confirms that initial exposure to low doses of O_3 produced only a partial, reversible oxidizing effect, resulting in a more stable antioxidant outcome. Because O_3 is a highly reactive gas composed of three oxygen atoms, we compared the effects of the two gases using the same protocol described previously, applying pure oxygen (O_2) and O_3 treatments. The experiment was performed using MRSA HI and DCF fluorescence intensity was measured after 20 minutes. As expected, since *Staphylococcus aureus* is an aerobic bacterium, O_2 MRSA HI had an oxidizing effect. As shown in Fig. 4, enhanced O_3 derived ROS production in both lymphoid (Fig. 4C) and monocytic (Fig. 4D) subpopulations is higher in the presence of O_3. Furthermore, it must be considered that O_2 does not inactivate bacteria unlike O_3.

3.6 Effects of O_3 on the Redox Status of MRSA-Treated PBMC

GSH plays a key role in maintaining the cellular redox balance by directly neutralizing ROS and serving as a cofactor for various enzymes. During this process, GSH is oxidized to oxidized glutathione (GSSG), which is then reduced back to GSH by specific enzymes. GSH is also essential for GPx activity, which protects cells from oxidative damage by reducing peroxides using GSH as an electron donor [54].

The increase in ROS formation in MRSA-treated PBMCs and the protective effects of O_3 prompted us to investigate the status of intracellular antioxidant defenses. It is well known that increased oxidative stress alters intracellular redox status due to the depletion of antioxidant defenses. Thus, we investigated the ability of O_3 to modulate the intracellular concentration of glutathione and the activity of the antioxidant enzyme GPx in unstimulated PBMCs or those activated with SEB as a positive control, MRSA O_3I, and MRSA HI (Fig. 5A). The GSH concentration was significantly decreased by SEB and by both MRSA O_3I and MRSA HI (Fig. 5A), indicating that the thiol was consumed in counteracting oxidant species formed in activated

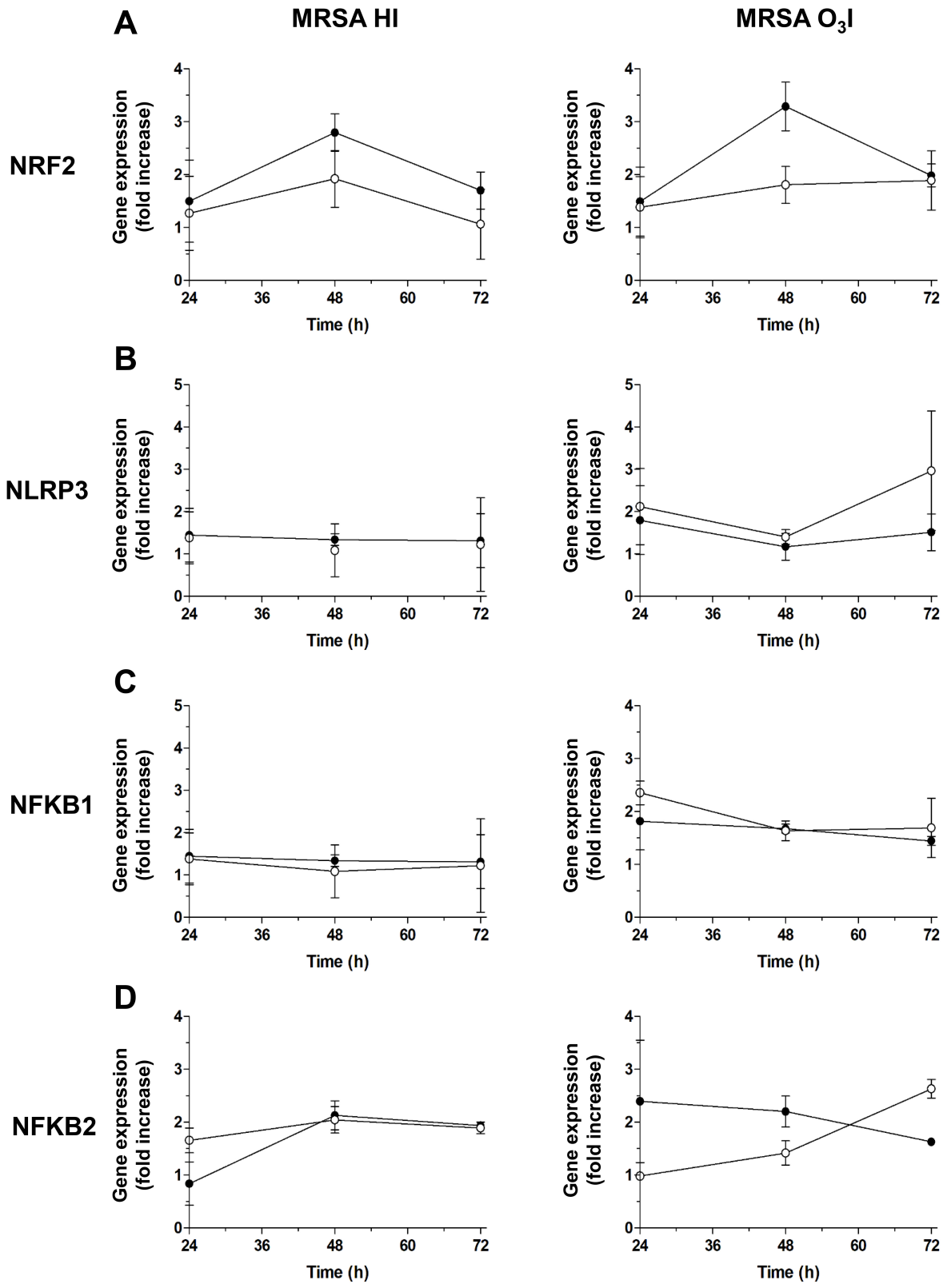


Fig. 3. Gene expression of key O_3 regulators. Graphs of the gene expression time course for key O_3 regulators assessed by RT-PCR from 24 to 72 hours: (A) antioxidant *NRF2*, (B) pro-oxidant *NLRP3,* (C) NF-κB, and its subunits *NFKB1* and *NFKB2* (D). A comparison is made between MRSA HI (left) and MRSA O_3I (right), before (white circles) and after (black circles) O_3 treatment. Results are expressed as fold changes in gene expression.

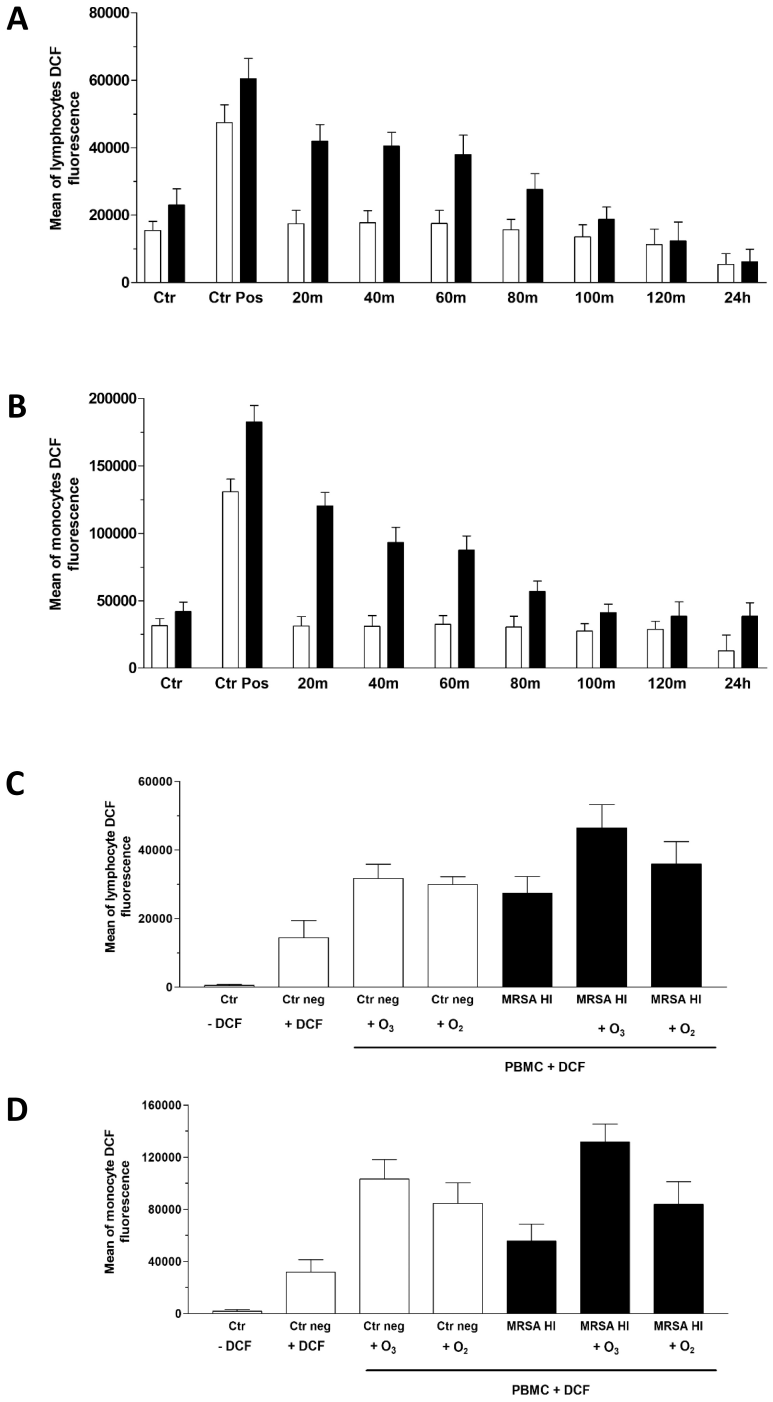


Fig. 4. Measurement of reactive oxygen species (ROS) via 2′,7′-Dichlorofluorescein (DCF) assay. Flow cytometry histograms of the ROS levels in PBMCs from MRSA-infected and non-infected samples treated with O_3. ROS production is measured at multiple time points (0–2 hours and 24 hours post-treatment) using the DCF assay. H_2O_2 was used as the positive control. Data are shown as the fluorescence intensity profiles for lymphocyte (A) and monocyte (B) populations. In panels (C) and (D) the comparison of ROS levels in MRSA-infected and non-infected PBMCs treated with O_3 or oxygen (O_2) was reported. ROS production has been assessed over time with the DCF assay. Statistical analysis was performed to compare the effects of O_3 and O_2 on ROS generation in lymphocytes (C) and monocytes (D), respectively. The experiments were conducted with five healthy subjects (see Raw data), but the figure presents descriptive statistics for a representative sample. Statistical analysis was performed to compare the effects of O_3 on ROS generation. The *p*-values for three experiments were significant in MRSA HI in both lymphocytes and monocytes. Data are described in (**Supplementary Table 2**). The *p*-value for three independent experiments, conducted by three different donors, was 0.075 (two-tailed) for paired samples comparing MRSA O_3I and DCF at 20 minutes, compared with MRSA O_3I and DCF at 24 hours (data not shown).

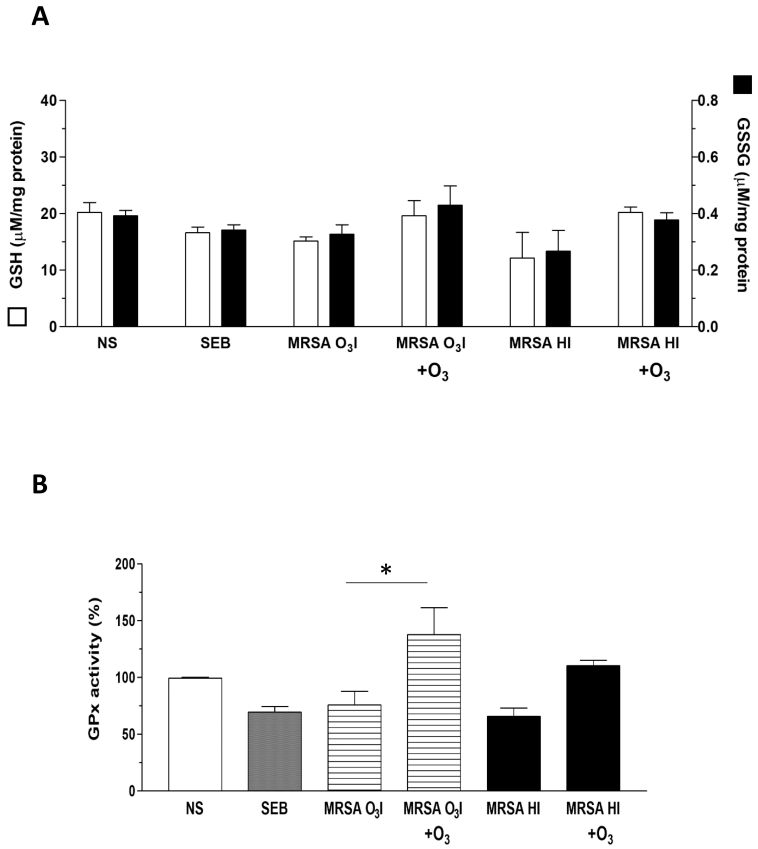


Fig. 5. Restoration of redox status in MRSA-treated PBMCs by ozone. (A) Graphs of the GSH and GSSG concentrations in PBMCs treated with SEB, MRSA O_3I, and MRSA HI. O_3 treatment is shown to restore redox balance to control-like levels. (B) GPx activity levels in PBMCs under various treatments, with data on the restorative effect of O_3 treatment. The results are presented as the mean $\pm$ SEM (n = 3), with statistical significance assessed by a paired *t*-test (*p*-value indicated). Data have been normalized to protein content (using the BCA protein assay). "*" indicates statistical significance determined by paired *t*-test (*$p \leq 0.05$).

PBMCs. Interestingly, the O_3 treatment restored GSH levels to levels comparable to controls when PBMCs were activated with MRSA O_3I and MRSA HI, whereas GSH levels were even higher than controls when activated with SEB.

The GSSG intracellular concentration was unaffected by the exposure of PBMCs to SEB or to MRSA O_3I; meanwhile, the GSSG intracellular concentration was significantly decreased by the MRSA HI treatment (Fig. 5A). The 40 µg/mL O_3 treatment did not significantly modify the GSSG concentration in any experimental condition tested with respect to the unstimulated cells or the corresponding treatment group.

The activity of GPx was significantly reduced in PBMCs activated with SEB or with MRSA O_3I and MRSA HI by 31, 25, and 35%, respectively, with respect to the unstimulated cells (Fig. 5B). In MRSA O_3I + O_3 versus MRSA O_3I, the difference was significant with a *p*-value of 0.026 for the two-tailed paired sample analysis. Interestingly, the 40 µg/mL O_3 treatment, not only restored but rather increased the enzyme activity in PBMCs activated with SEB or with MRSA O_3I and MRSA HI by 24, 37 and 10%, respectively, compared to the unstimulated cells (Fig. 5B). Overall, these results show that O_3, can protect cells from MRSA-dependent oxidative stress, decreasing the levels of ROS formed and restoring the intracellular redox equilibrium.

4. Discussion

This *in vitro* study highlights the potential of O_3 therapy as a complementary strategy for managing *Staphylococcus aureus* infections, particularly MRSA, which poses a serious challenge due to the associated resistance to conventional antibiotics. Notably, O_3 demonstrated a dual effect: direct bactericidal activity against MRSA and significant immunomodulatory and antioxidant effects on human PBMCs.

MRSA, when inactivated by a single-step O_3 treatment in PBS, induced a pro-inflammatory response in PBMCs, as evidenced by cytokine production within 24 hours. However, subsequent addition of O_3 to the cultures led to a marked reduction in both intracellular and secreted pro-inflammatory cytokines, as shown by the ICS and CBA assays, respectively, indicating an anti-inflammatory effect. This trend was also observed with heat-inactivated bacte-

ria, suggesting that the immunomodulatory response is influenced more by bacterial viability than by the inactivation method [48]. An intriguing discrepancy emerged in IL-10 levels between ICS and CBA measurements. Indeed, while IL-10 levels consistently decreased in the CBA assay, these levels increased in the ICS assay. This pattern was evident under both O_3-inactivated and heat-inactivated bacterial conditions. This effect was particularly evident in the CD3+ and CD8+ T cell subsets, whereas IL-10 levels remained stable in CD4+ lymphocytes. Given that IL-10 is an O_3-induced anti-inflammatory mediator, this finding warrants further investigation [55]. One possible explanation is that the early time point (24 hours), may be sufficient to detect intracellular IL-10 synthesis but not secretion. Additionally, differential responses between CD4+ and CD8+ cells may indicate an effect of O_3 on other immune subsets such as CD3– NK cells (CD56+), double-negative T cells (CD3+CD4–CD8–), or Tregs, which warrants further investigation. These cells, which can be either CD4+ or CD8+, play a role in maintaining homeostasis, preventing autoimmunity [56] and reducing exacerbation of CD8+ lymphocyte responses to pathogens, thereby helping to restore the integrity of damaged tissues [57].

A general decrease in IFN-γ and IL-4 within ICS further supports an anti-inflammatory shift, while IL-17 levels decreased in CD3+ and CD4+ cells but increased in CD8+ T cells. This dual role of IL-17 is notable, as it may exhibit pro-inflammatory or tissue-repairing properties depending on the context—particularly in the presence of IL-10, as seen in mucosal environments [58]. Moreover, IL-17, which Tregs also produce, plays an important role in controlling microbial inflammation at mucosal sites, and autoimmunity, and also in activating the innate immune response through neutrophil activation [59].

The slight increase in IL-8 secretion, despite the general reduction in TNF-α, IL-6, IL-1β, and IL-10, supports the hypothesis that IL-8 may have a reparative or immunosuppressive role, possibly associated with M2 macrophage polarization, and aligns with previous studies showing IL-8 elevation following O_3 exposure [60,61].

At the molecular level, qRT-PCR data demonstrated activation of the NRF2-KEAP1 antioxidant pathway by 48 hours, accompanied by downregulation of NLRP3 and NFKB1—key mediators of the inflammatory response, thereby confirming that O_3 may exert antioxidant and immunomodulatory effects. Interestingly, NFKB2 exhibited a divergent pattern in response to MRSA HI stimulation, being upregulated 48 hours after O_3 treatment and subsequently downregulated at 72 hours. This pattern suggests differential regulation of NF-κB heterodimers, with potential implications for transcriptional activity and inflammatory signaling.

With respect to oxidative stress, our data confirmed that MRSA induces significant ROS generation, which is rapidly reduced by O_3 treatment within 24 hours, as previously described both *in vitro* [62,63] and *in vivo* [64–66] models. This was accompanied by a restoration of the intracellular redox balance, likely mediated by activation of the AMPK/Keap1/Nrf2 axis. This pathway promotes transcription of antioxidant response element (ARE)-regulated genes such as GCLC and GPx, thereby enhancing GSH synthesis and antioxidant enzyme activity [67]. Overall, this study demonstrates, using biochemical, immunological, and molecular approaches, that O_3 exerts rapid and sustained anti-inflammatory and antioxidant effects, with maximal impact observed between 48–72 hours post-treatment. These findings underscore the potential of O_3 as a supportive therapy for multidrug-resistant infections such as MRSA.

5. Conclusions

This pilot study suggests that O_3 therapy exerts antibacterial, antioxidant, and immunomodulatory effects on MRSA-stimulated PBMCs. These findings support the potential use of O_3 therapy as an adjunct strategy to combat antimicrobial resistance and warrant further validation in more advanced models.

6. Future Directions

Although the limited number of PBMC donors presents a challenge, the consistent and reproducible patterns observed across all experimental methods, except for qRT-PCR at 24 hours, indicate a robust and non-random response. Future research should include a larger donor pool and examine additional cell subsets, such as Tregs, NK cells, and double-negative T cells, to further elucidate the cellular targets potentially affected by O_3. Additionally, extending time-course analyses beyond 24 hours will be crucial for clarifying the kinetics of cytokine secretion, particularly IL-10, IL-17A, and IL-8.

Availability of Data and Materials

The analyzed data sets generated during the study are available from the corresponding author upon request.

Author Contributions

AC: Conceptualization and Project design, supervision, funding acquisition, data curation and writing—original draft. CC: Development of techniques for cell ozonation, investigation, data analysis, writing—review and editing. VLS: Investigation, validation, writing—review and editing. IM: Investigation, validation, data analysis, writing—original draft, and writing—review and editing. SG: Development of techniques for bacterial cells ozonation, investigation and techniques validation; data analysis, writing and editing. MP: Development of techniques for bacterial cells ozonation, investigation and techniques validation; data analysis, writing and editing. DP: Investigation, data curation, writing—review and editing.

MS: Supervision (cellular group), methodology, validation, writing—review and editing, data curation. MZ: Investigation, methodology, and validation. GC: Investigation, methodology, and data curation. MFab: Investigation, methodology, and data curation. MM: Conceptualization, supervision, methodology, validation, data curation, writing, and editing. MDG: Conceptualization, supervision, methodology, validation, data curation, writing, and editing. RC: Conceptualization, supervision, methodology, validation, data curation, writing, and editing. GE: Conceptualization, supervision, methodology, validation, data curation, writing, and editing. SP: Conceptualization support, data interpretation, and visualization. LV and MFra: Literature search, provision of the MultiOssigen 99 IR device, funding acquisition, and project administration. All authors contributed to editorial changes in the manuscript. All authors read and approved the final version of manuscript and have participated sufficiently in the work and agreed to be accountable for all aspects of the work.

Ethics Approval and Consent to Participate

This study was approved by the Ethics Committee of the Italian National Institute of Health with protocol PRE BIO CE n.0041072 approved on 24/11/2021, and has been conducted in accordance with the Declaration of Helsinki. Human PBMCs were isolated from freshly collected buffy coats derived from healthy male and female volunteers (Blood Bank of University "La Sapienza", Rome, Italy) that gave written informed consent.

Acknowledgment

We thank all our colleagues of the Italian National Institute of Health, Rome, Italy. In particular, Eliana Coccia and Marilena Etna for their valuable assistance and helpful discussion; Alessandro Giuliani for his important support in statistical analysis; Simone Martinelli and Giuseppe Esposito for their advice and assistance in use of the gamma-ray technique; Fabio D'Ambrosio for his aid in bacterial collection. We thank Massimo Delle Femmine for improving the figures quality.

Funding

This work was supported by SIOOT project funding number BB08.

Conflicts of Interest

The authors declare no conflicts of interest.

Supplementary Material

Supplementary material associated with this article can be found, in the online version, at https://doi.org/10.31083/FBE44093.

References

[1] Smith AM, Ramudzulu M, Munk P, Avot BJP, Esterhuyse KCM, van Blerk N, *et al*. Metagenomics analysis of sewage for surveillance of antimicrobial resistance in South Africa. PLoS ONE. 2024; 19: e0309409. https://doi.org/10.1371/journal.pone.0309409.

[2] Hendriksen RS, Munk P, Njage P, van Bunnik B, McNally L, Lukjancenko O, *et al*. Global monitoring of antimicrobial resistance based on metagenomics analyses of urban sewage. Nature Communications. 2019; 10: 1124. https://doi.org/10.1038/s41467-019-08853-3.

[3] Song M, Zeng Q, Xiang Y, Gao L, Huang J, Huang J, *et al*. The antibacterial effect of topical ozone on the treatment of MRSA skin infection. Molecular Medicine Reports. 2018; 17: 2449–2455. https://doi.org/10.3892/mmr.2017.8148.

[4] Monaco M, Pimentel de Araujo F, Cruciani M, Coccia EM, Pantosti A. Worldwide Epidemiology and Antibiotic Resistance of Staphylococcus aureus. In Bagnoli F, Rappuoli R, Grandi G (eds.) Staphylococcus aureus: Microbiology, Pathology, Immunology, Therapy and Prophylaxis (pp. 21–56). Springer International Publishing: Cham. 2016. https://doi.org/10.1007/82_2016_3.

[5] Sousa SA, Feliciano JR, Pita T, Soeiro CF, Mendes BL, Alves LG, *et al*. Bacterial Nosocomial Infections: Multidrug Resistance as a Trigger for the Development of Novel Antimicrobials. Antibiotics (Basel, Switzerland). 2021; 10: 942. https://doi.org/10.3390/antibiotics10080942.

[6] Ozturk B, Kurtoglu T, Durmaz S, Kozaci LD, Abacigil F, Ertugrul B, *et al*. The effects of ozone on bacterial growth and thiol-disulphide homeostasis in vascular graft infection caused by MRSA in rats. Acta Cirurgica Brasileira. 2017; 32: 219–228. https://doi.org/10.1590/S0102-865020170030000006.

[7] Franzini M, Valdenassi L, Pandolfi S, Tirelli U, Ricevuti G, Chirumbolo S. The Role of Ozone as an Nrf2-Keap1-ARE Activator in the Anti-Microbial Activity and Immunity Modulation of Infected Wounds. Antioxidants (Basel, Switzerland). 2023; 12: 1985. https://doi.org/10.3390/antiox12111985.

[8] Chirumbolo S, Valdenassi L, Tirelli U, Pandolfi S, Franzini M. The use of the medical ozone in the immune challenge of multidrug resistant (MDR) bacteria and the role of mitochondria. Microbes and Infection. 2024; 26: 105242. https://doi.org/10.1016/j.micinf.2023.105242.

[9] Azuma T, Katagiri M, Sekizuka T, Kuroda M, Watanabe M. Inactivation of Bacteria and Residual Antimicrobials in Hospital Wastewater by Ozone Treatment. Antibiotics (Basel, Switzerland). 2022; 11: 862. https://doi.org/10.3390/antibiotics11070862.

[10] Baghal Asghari F, Dehghani MH, Dehghanzadeh R, Farajzadeh D, Shanehbandi D, Mahvi AH, *et al*. Performance evaluation of ozonation for removal of antibiotic-resistant Escherichia coli and Pseudomonas aeruginosa and genes from hospital wastewater. Scientific Reports. 2021; 11: 24519. https://doi.org/10.1038/s41598-021-04254-z.

[11] Fontes B, Cattani Heimbecker AM, de Souza Brito G, Costa SF, van der Heijden IM, Levin AS, *et al*. Effect of low-dose gaseous ozone on pathogenic bacteria. BMC Infectious Diseases. 2012; 12: 358. https://doi.org/10.1186/1471-2334-12-358.

[12] Gulmen S, Kurtoglu T, Meteoglu I, Kaya S, Okutan H. Ozone therapy as an adjunct to vancomycin enhances bacterial elimination in methicillin resistant Staphylococcus aureus mediastinitis. The Journal of Surgical Research. 2013; 185: 64–69. https://doi.org/10.1016/j.jss.2013.05.085.

[13] Silva V, Peirone C, Amaral JS, Capita R, Alonso-Calleja C, Marques-Magallanes JA, *et al*. High Efficacy of Ozonated Oils on the Removal of Biofilms Produced by Methicillin-Resistant

Staphylococcus aureus (MRSA) from Infected Diabetic Foot Ulcers. Molecules (Basel, Switzerland). 2020; 25: 3601. https://doi.org/10.3390/molecules25163601.

[14] Sagai M, Bocci V. Mechanisms of Action Involved in Ozone Therapy: Is healing induced via a mild oxidative stress? Medical Gas Research. 2011; 1: 29. https://doi.org/10.1186/2045-9912-1-29.

[15] Yang J, Luo K, Chen ZJ, Zhang GH, Yao X, Feng SX, *et al*. Clinical efficacy and metabolomic analysis of ozone major autohemotherapy for the treatment of herpes zoster. Postepy Dermatologii i Alergologii. 2023; 40: 693–698. https://doi.org/10.5114/ada.2023.130522.

[16] Skomro P, Opalko K, Gadomska-Krasny J, Lietz-Kijak D, Perzanowska-Stefańska M. Ozone therapy with the OzonyTron apparatus. Annales Academiae Medicae Stetinensis. 2005; 51: 39–42.

[17] Izadi M, Cegolon L, Javanbakht M, Sarafzadeh A, Abolghasemi H, Alishiri G, *et al*. Ozone therapy for the treatment of COVID-19 pneumonia: A scoping review. International Immunopharmacology. 2021; 92: 107307. https://doi.org/10.1016/j.intimp.2020.107307.

[18] Radvar S, Karkon-Shayan S, Motamed-Sanaye A, Majidi M, Hajebrahimi S, Taleschian-Tabrizi N, *et al*. Using Ozone Therapy as an Option for Treatment of COVID-19 Patients: A Scoping Review. Advances in Experimental Medicine and Biology. 2021; 1327: 151–160. https://doi.org/10.1007/978-3-030-71697-4_12.

[19] Jafari-Oori M, Vahedian-Azimi A, Ghorbanzadeh K, Sepahvand E, Dehi M, Ebadi A, *et al*. Efficacy of ozone adjuvant therapy in COVID-19 patients: A meta-analysis study. Frontiers in Medicine. 2022; 9: 1037749. https://doi.org/10.3389/fmed.2022.1037749.

[20] Chirumbolo S, Varesi A, Franzini M, Valdenassi L, Pandolfi S, Tirelli U, *et al*. The Mito-Hormetic Mechanisms of Ozone in the Clearance of SARS-CoV2 and in the COVID-19 Therapy. Biomedicines. 2022; 10: 2258. https://doi.org/10.3390/biomedicines10092258.

[21] Cenci A, Macchia I, La Sorsa V, Sbarigia C, Di Donna V, Pietraforte D. Mechanisms of Action of Ozone Therapy in Emerging Viral Diseases: Immunomodulatory Effects and Therapeutic Advantages With Reference to SARS-CoV-2. Frontiers in Microbiology. 2022; 13: 871645. https://doi.org/10.3389/fmicb.2022.871645.

[22] Chirumbolo S, Valdenassi L, Simonetti V, Bertossi D, Ricevuti G, Franzini M, *et al*. Insights on the mechanisms of action of ozone in the medical therapy against COVID-19. International Immunopharmacology. 2021; 96: 107777. https://doi.org/10.1016/j.intimp.2021.107777.

[23] Cattel F, Giordano S, Bertiond C, Lupia T, Corcione S, Scaldaferri M, *et al*. Ozone therapy in COVID-19: A narrative review. Virus Research. 2021; 291: 198207. https://doi.org/10.1016/j.virusres.2020.198207.

[24] Yousefi B, Banihashemian SZ, Feyzabadi ZK, Hasanpour S, Kokhaei P, Abdolshahi A, *et al*. Potential therapeutic effect of oxygen-ozone in controlling of COVID-19 disease. Medical Gas Research. 2022; 12: 33–40. https://doi.org/10.4103/2045-9912.325989.

[25] Bocci V, Borrelli E, Travagli V, Zanardi I. The ozone paradox: ozone is a strong oxidant as well as a medical drug. Medicinal Research Reviews. 2009; 29: 646–682. https://doi.org/10.1002/med.20150.

[26] Xue W, Macleod J, Blaxland J. The Use of Ozone Technology to Control Microorganism Growth, Enhance Food Safety and Extend Shelf Life: A Promising Food Decontamination Technology. Foods (Basel, Switzerland). 2023; 12: 814. https://doi.org/10.3390/foods12040814.

[27] Epelle EI, Macfarlane A, Cusack M, Burns A, Okolie JA, Mackay W, *et al*. Ozone application in different industries: A review of recent developments. Chemical Engineering Journal (Lausanne, Switzerland: 1996). 2023; 454: 140188. https://doi.org/10.1016/j.cej.2022.140188.

[28] Burgassi S, Zanardi I, Travagli V, Montomoli E, Bocci V. How much ozone bactericidal activity is compromised by plasma components? Journal of Applied Microbiology. 2009; 106: 1715–1721. https://doi.org/10.1111/j.1365-2672.2008.04141.x.

[29] Tricarico G, Travagli V. The Relationship between Ozone and Human Blood in the Course of a Well-Controlled, Mild, and Transitory Oxidative Eustress. Antioxidants (Basel, Switzerland). 2021; 10: 1946. https://doi.org/10.3390/antiox10121946.

[30] Cai Y, Zhao Y, Wang C, Yadav AK, Wei T, Kang P. Ozone disinfection of waterborne pathogens: A review of mechanisms, applications, and challenges. Environmental Science and Pollution Research International. 2024; 31: 60709–60730. https://doi.org/10.1007/s11356-024-34991-3.

[31] Rangel K, Cabral FO, Lechuga GC, Carvalho JPRS, Villas-Bôas MHS, Midlej V, *et al*. Potent Activity of a High Concentration of Chemical Ozone against Antibiotic-Resistant Bacteria. Molecules (Basel, Switzerland). 2022; 27: 3998. https://doi.org/10.3390/molecules27133998.

[32] Westover C, Rahmatulloev S, Danko D, Afshin EE, O'Hara NB, Ounit R, *et al*. Ozone Disinfection for Elimination of Bacteria and Degradation of SARS-CoV2 RNA for Medical Environments. Genes. 2023; 14: 85. https://doi.org/10.3390/genes14010085.

[33] Murray BK, Ohmine S, Tomer DP, Jensen KJ, Johnson FB, Kirsi JJ, *et al*. Virion disruption by ozone-mediated reactive oxygen species. Journal of Virological Methods. 2008; 153: 74–77. https://doi.org/10.1016/j.jviromet.2008.06.004.

[34] Chirumbolo S, Valdenassi L, Tirelli U, Ricevuti G, Pandolfi S, Vaiano F, *et al*. The Oxygen-Ozone Adjunct Medical Treatment According to the Protocols from the Italian Scientific Society of Oxygen-Ozone Therapy: How Ozone Applications in the Blood Can Influence Clinical Therapy Success via the Modulation of Cell Biology and Immunity. Biology. 2023; 12: 1512. https://doi.org/10.3390/biology12121512.

[35] Chen ZH, Saito Y, Yoshida Y, Sekine A, Noguchi N, Niki E. 4-Hydroxynonenal induces adaptive response and enhances PC12 cell tolerance primarily through induction of thioredoxin reductase 1 via activation of Nrf2. The Journal of Biological Chemistry. 2005; 280: 41921–41927. https://doi.org/10.1074/jbc.M508556200.

[36] Bocci VA, Zanardi I, Travagli V. Ozone acting on human blood yields a hormetic dose-response relationship. Journal of Translational Medicine. 2011; 9: 66. https://doi.org/10.1186/1479-5876-9-66.

[37] Galiè M, Covi V, Tabaracci G, Malatesta M. The Role of Nrf2 in the Antioxidant Cellular Response to Medical Ozone Exposure. International Journal of Molecular Sciences. 2019; 20: 4009. https://doi.org/10.3390/ijms20164009.

[38] Smith NL, Wilson AL, Gandhi J, Vatsia S, Khan SA. Ozone therapy: an overview of pharmacodynamics, current research, and clinical utility. Medical Gas Research. 2017; 7: 212–219. https://doi.org/10.4103/2045-9912.215752.

[39] Cheng YW, Liu J, Finkel T. Mitohormesis. Cell Metabolism. 2023; 35: 1872–1886. https://doi.org/10.1016/j.cmet.2023.10.011.

[40] Kasai S, Shimizu S, Tatara Y, Mimura J, Itoh K. Regulation of Nrf2 by Mitochondrial Reactive Oxygen Species in Physiology and Pathology. Biomolecules. 2020; 10: 320. https://doi.org/10.3390/biom10020320.

[41] Delgado-Roche L, Riera-Romo M, Mesta F, Hernández-Matos Y, Barrios JM, Martínez-Sánchez G, *et al*. Medical ozone pro-

motes Nrf2 phosphorylation reducing oxidative stress and pro-inflammatory cytokines in multiple sclerosis patients. European Journal of Pharmacology. 2017; 811: 148–154. https://doi.org/10.1016/j.ejphar.2017.06.017.

[42] Guo H, Callaway JB, Ting JPY. Inflammasomes: mechanism of action, role in disease, and therapeutics. Nature Medicine. 2015; 21: 677–687. https://doi.org/10.1038/nm.3893.

[43] Yu G, Bai Z, Chen Z, Chen H, Wang G, Wang G, *et al*. The NLRP3 inflammasome is a potential target of ozone therapy aiming to ease chronic renal inflammation in chronic kidney disease. International Immunopharmacology. 2017; 43: 203–209. https://doi.org/10.1016/j.intimp.2016.12.022.

[44] Kamada N, Seo SU, Chen GY, Núñez G. Role of the gut microbiota in immunity and inflammatory disease. Nature Reviews. Immunology. 2013; 13: 321–335. https://doi.org/10.1038/nri3430.

[45] Tahmasebi S, Qasim MT, Krivenkova MV, Zekiy AO, Thangavelu L, Aravindhan S, *et al*. The effects of oxygen-ozone therapy on regulatory T-cell responses in multiple sclerosis patients. Cell Biology International. 2021; 45: 1498–1509. https://doi.org/10.1002/cbin.11589.

[46] Correa W, Brandenburg J, Behrends J, Heinbockel L, Reiling N, Paulowski L, *et al*. Inactivation of Bacteria by γ-Irradiation to Investigate the Interaction with Antimicrobial Peptides. Biophysical Journal. 2019; 117: 1805–1819. https://doi.org/10.1016/j.bpj.2019.10.012.

[47] Anello P, Esposito G. Biological effects in normal human fibroblasts following chronic and acute irradiation with both low- and high-LET radiation. Frontiers in Public Health. 2024; 12: 1404748. https://doi.org/10.3389/fpubh.2024.1404748.

[48] Cruciani M, Sandini S, Etna MP, Giacomini E, Camilli R, Severa M, *et al*. Differential Responses of Human Dendritic Cells to Live or Inactivated *Staphylococcus aureus*: Impact on Cytokine Production and T Helper Expansion. Frontiers in Immunology. 2019; 10: 2622. https://doi.org/10.3389/fimmu.2019.02622.

[49] Macchia I, La Sorsa V, Ruspantini I, Sanchez M, Tirelli V, Carollo M, *et al*. Multicentre Harmonisation of a Six-Colour Flow Cytometry Panel for Naïve/Memory T Cell Immunomonitoring. Journal of Immunology Research. 2020; 2020: 1938704. https://doi.org/10.1155/2020/1938704.

[50] Alhede M, Kragh KN, Qvortrup K, Allesen-Holm M, van Gennip M, Christensen LD, *et al*. Phenotypes of non-attached Pseudomonas aeruginosa aggregates resemble surface attached biofilm. PLoS ONE. 2011; 6: e27943. https://doi.org/10.1371/journal.pone.0027943.

[51] Reisz JA, Bansal N, Qian J, Zhao W, Furdui CM. Effects of ionizing radiation on biological molecules–mechanisms of damage and emerging methods of detection. Antioxidants & Redox Signaling. 2014; 21: 260–292. https://doi.org/10.1089/ars.2013.5489.

[52] Fertey J, Bayer L, Grunwald T, Pohl A, Beckmann J, Gotzmann G, *et al*. Pathogens Inactivated by Low-Energy-Electron Irradiation Maintain Antigenic Properties and Induce Protective Immune Responses. Viruses. 2016; 8: 319. https://doi.org/10.3390/v8110319.

[53] Halliwell B, Gutteridge JMC. Free Radicals in Biology and Medicine. Oxford University Press: Oxford. 2015.

[54] Hatem E, El Banna N, Huang ME. Multifaceted Roles of Glutathione and Glutathione-Based Systems in Carcinogenesis and Anticancer Drug Resistance. Antioxidants & Redox Signaling. 2017; 27: 1217–1234. https://doi.org/10.1089/ars.2017.7134.

[55] Backus GS, Howden R, Fostel J, Bauer AK, Cho HY, Marzec J, *et al*. Protective role of interleukin-10 in ozone-induced pulmonary inflammation. Environmental Health Perspectives. 2010; 118: 1721–1727. https://doi.org/10.1289/ehp.1002182.

[56] Mishra S, Srinivasan S, Ma C, Zhang N. $CD8^+$ Regulatory T Cell - A Mystery to Be Revealed. Frontiers in Immunology. 2021; 12: 708874. https://doi.org/10.3389/fimmu.2021.708874.

[57] Vieyra-Lobato MR, Vela-Ojeda J, Montiel-Cervantes L, López-Santiago R, Moreno-Lafont MC. Description of $CD8^+$ Regulatory T Lymphocytes and Their Specific Intervention in Graft-versus-Host and Infectious Diseases, Autoimmunity, and Cancer. Journal of Immunology Research. 2018; 2018: 3758713. https://doi.org/10.1155/2018/3758713.

[58] Manuzak J, Dillon S, Wilson C. Differential interleukin-10 (IL-10) and IL-23 production by human blood monocytes and dendritic cells in response to commensal enteric bacteria. Clinical and Vaccine Immunology: CVI. 2012; 19: 1207–1217. https://doi.org/10.1128/CVI.00282-12.

[59] Voo KS, Wang YH, Santori FR, Boggiano C, Wang YH, Arima K, *et al*. Identification of IL-17-producing FOXP3+ regulatory T cells in humans. Proceedings of the National Academy of Sciences of the United States of America. 2009; 106: 4793–4798. https://doi.org/10.1073/pnas.0900408106.

[60] Bocci V, Valacchi G, Corradeschi F, Fanetti G. Studies on the biological effects of ozone: 8. Effects on the total antioxidant status and on interleukin-8 production. Mediators of Inflammation. 1998; 7: 313–317. https://doi.org/10.1080/09629359890820.

[61] Malatesta M, Cisterna B, Costanzo M. Cellular and Molecular Mechanisms of Ozone Therapy: Present Knowledge and Prospective Applications. International Journal of Molecular Sciences. 2022; 23: 12586. https://doi.org/10.3390/ijms232012586.

[62] Luo Z, Wang Q, Fan X, Koh XQ, Loh XJ, Wu C, *et al*. ROS-Driven Nanoventilator for MRSA-Induced Acute Lung Injury Treatment via In Situ Oxygen Supply, Anti-Inflammation and Immunomodulation. Advanced Science (Weinheim, Baden-Wurttemberg, Germany). 2025; 12: e2406060. https://doi.org/10.1002/advs.202406060.

[63] Rangel K, Cabral FO, Lechuga GC, Carvalho JPRS, Villas-Bôas MHS, Midlej V, *et al*. Potent Activity of a High Concentration of Chemical Ozone against Antibiotic-Resistant Bacteria. Molecules (Basel, Switzerland). 2022; 27: 3998. https://doi.org/10.3390/molecules27133998.

[64] Chakraborty SP, Mahapatra SK, Roy S. In vitro time-dependent vancomycin-resistant Staphylococcus aureus-induced free radical generation and status of antioxidant enzymes in murine peritoneal macrophage. Toxicology Mechanisms and Methods. 2012; 22: 9–22. https://doi.org/10.3109/15376516.2011.583296.

[65] Long N, Zhang Y, Qiu M, Deng J, Sun F, Dai M. Dynamic changes of inflammatory response and oxidative stress induced by methicillin-resistant Staphylococcus aureus in mice. European Journal of Clinical Microbiology & Infectious Diseases: Official Publication of the European Society of Clinical Microbiology. 2022; 41: 79–86. https://doi.org/10.1007/s10096-021-04349-5.

[66] Tang H, Long N, Lin L, Liu Y, Li J, Sun F, *et al*. Effect of MRSA on CYP450: dynamic changes of cytokines, oxidative stress, and drug-metabolizing enzymes in mice infected with MRSA. Infection and Drug Resistance. 2018; 11: 229–238. https://doi.org/10.2147/IDR.S153871.

[67] Clavo B, Martínez-Sánchez G, Rodríguez-Esparragón F, Rodríguez-Abreu D, Galván S, Aguiar-Bujanda D, *et al*. Modulation by Ozone Therapy of Oxidative Stress in Chemotherapy-Induced Peripheral Neuropathy: The Background for a Randomized Clinical Trial. International Journal of Molecular Sciences. 2021; 22: 2802. https://doi.org/10.3390/ijms22062802.